Correlation of Arrhenius behaviors in power and capacity fades with cell impedance and heat generation in cylindrical lithium-ion cells

Bor Yann Liaw[1], E. Peter Roth, Rudolph G. Jungst,
Ganesan Nagasubramanian, Herbert L. Case, Daniel H. Doughty[*]

Lithium Battery R&D Department, Sandia National Laboratories, P.O. Box 5800, MS-0613, Albuquerque, NM 87185, USA

Abstract

A series of cylindrical 18650 lithium-ion cells with an MAG-10|1.2 M LiPF$_6$ ethylene carbonate (EC):ethyl methyl carbonate (EMC) (w:w = 3:7)|Li$_x$Ni$_{0.8}$Co$_{0.15}$Al$_{0.05}$O$_2$ configuration were made and tested for power-assist hybrid electric vehicle (HEV) applications under various aging conditions of temperature and state-of-charge (SOC). The cells were intermittently characterized for changes in power capability, rate capacity, and impedance as aging progressed. The changes of these properties with temperature, as depicted by Arrhenius equations, were analyzed. We found that the degradation in power and capacity fade seems to relate to the impedance increase in the cell. The degradation follows a multi-stage process. The initial stage of degradation has an activation energy of the order of 50–55 kJ/mol, as derived from power fade and C_1 capacity fade measured at $C/1$ rate. In addition, microcalorimetry was performed on two separate unaged cells at 80% SOC at various temperatures to measure static heat generation in the cells. We found that the static heat generation has an activation energy of the order of 48–55 kJ/mol, similar to those derived from power and C_1 capacity fade. The correspondence in the magnitude of the activation energy suggests that the power and C_1 capacity fades were related to the changes of the impedance in the cells, most likely via the same fading mechanism. The fading mechanism seemed to be related to the static heat generation of the cell.
© 2003 Published by Elsevier Science B.V.

Keywords: Lithium-ion battery; Li$_x$Ni$_{0.8}$Co$_{0.15}$Al$_{0.05}$O$_2$ cathode; Accelerated life tests; Arrhenius plots; Activation energy

1. Introduction

Lithium-ion batteries have experienced rapid acceptance for use in consumer electronics. Similar technologies are also being considered for transportation applications such as in the hybrid electric vehicles (HEV). Calendar and cycle life of these batteries are therefore an important concern that needs to be assessed and addressed. Under the US Department of Energy's (DOE) Advanced Technology Development (ATD) Program, there is a collective effort between US auto industry and five DOE national laboratories to develop advanced lithium-ion battery technology for power-assist HEV applications. Sandia National Laboratories have been involved in the investigation of accelerated life tests (ALT) to determine battery life and to develop predictive models [1].

In the accelerated life tests, the cells were exposed to different temperatures for thermal aging. In our tests, four different temperatures (25, 35, 45, and 55 °C) were used. The degradation from thermal aging was estimated from the cells by gauging, for example the power capability loss (PCL, power fade) or capacity loss (capacity fade) as a function of aging conditions. The cells were also subjected to aging at different states-of-charge (SOC), so degradation on composition dependence was assessed. Three different SOCs at 60, 80 and 100% were investigated in this work. The cells were also subjected to cycling, so that their dependence on cycling conditions was investigated as well.

The thermal aging provides the basis for Arrhenius type analysis of the thermally activated process in the degradation.

---

[*] Corresponding author. Tel.: +1-505-845-8105; fax: +1-505-844-6972.
E-mail addresses: bliaw@hawaii.edu (B.Y. Liaw), dhdough@sandia.gov (D.H. Doughty).
[1] On leave from Hawaii Natural Energy Institute, School of Ocean and Earth Science and Technology, University of Hawaii at Manoa, Honolulu, Hawaii.

Arrhenius behavior is depicted by the well-known Arrhenius equation, typically expressed as

$$A = A_0 \exp\left(-\frac{E_a}{RT}\right) \tag{1}$$

where A is a quantity of interest, typically related to the rate of change of the property in the system, which is thermally activated; A_0 a pre-exponential term, depicting an intrinsic value of such a property; E_a the activation energy representing the energy barrier for the thermal activation process; R the universal gas constant; and, T the absolute temperature in Kelvin. The activation energy related to these properties can be derived from the slope of the corresponding Arrhenius plot in which the quantity of these properties in a logarithmic scale is plotted against the reciprocal temperature and a linear slope is usually observed. What will be discussed in this paper is the correlation among the Arrhenius behaviors derived from power fade, capacity fade, impedance change, and static heat generation. The information derived from this work can assist the understanding of the fading mechanisms and the prediction of battery life using accelerated life tests. Detailed diagnostic characterization of the fading mechanisms is in progress.

2. Experimental

A series of cylindrical 18650 lithium-ion cells with an MAG-10|1.2 M LiPF$_6$ ethylene carbonate (EC):ethyl methyl carbonate (EMC) (w:w = 3:7)|Li$_x$Ni$_{0.8}$Co$_{0.15}$Al$_{0.05}$O$_2$ configuration were made by Quallion (Sylmar, CA) with special tap design to deliver high power (herein we called GEN 2 cells). The test procedures are described in the partnership of new generation vehicles (PNGV) test manual developed by the US Department of Energy [2]. The cells are typically stored at 10 °C when they are not being subjected to the aging tests. For accelerated life tests, three to five cells are usually used and subjected to the same test condition under thermal stress to accelerate degradation. At 4-week intervals during aging, the cells are brought to 25 °C for reference performance tests (RPT), which include hybrid pulse power characterization (HPPC), rate capacity determination at $C/1$ and $C/25$ rates, and ac electrochemical impedance spectroscopy (EIS) measurements, as described in the test manual [2]. When the cells meet the end of test (EOT) condition, they are removed from aging. The data presented here cover as long as 36 weeks of aging for some of the lower temperature aged cells, while some of the higher temperature higher-SOC aged cells were retired as early as 20 weeks.

The power fade reported here is estimated from the characterization of power capability determined by the HPPC. The HPPC typically tests cells at 10% SOC intervals with a 5C 18-s discharge pulse, a 32-s rest, and a 3.75C 10-s

regenerative pulse, within the voltage range of 3.0 and 4.3 V. The hybrid power capability is estimated from scaling the cell test result with a battery size factor to meet the PNGV goal of 300 Wh for power-assist HEV application. The power fade is reported in reflecting the percentage drop in power capability in each RPT from the value determined at the beginning of life (BOL; usually within 2 weeks prior to commencing life tests). The capacity fade is reported also in percentage, showing the decrease in rate capacity from the value determined at the BOL. The interfacial impedance reported here is the width of the semicircle or arc often shown up in the middle frequency range in the NyQuist plot, usually referred to originating from charge transfer. The change in impedance refers to the difference in impedance in each RPT from the value determined at the BOL.

3. Results and discussion

The power degradation behavior observed in the GEN 2 cells that went through different stages of thermal aging at different SOCs and durations is shown in Fig. 1, which illustrates the time- and temperature-dependent aging behavior related to the power fade found in HPPC after each RPT. The most intriguing feature that we found in the power degradation is the distinct slopes in the percentage power fade versus logarithmic time curves for all SOCs, as shown in Fig. 2. The symbols are averaged power fade values measured from RPTs at each 4-week interval of aging. The solid lines represent a series of linear curve fittings with the best fit subjectively selected over a region on the curve. The region that shares a common slope is considered dominated by the same degradation process. The presence of multiple distinct slopes on each curve suggests that the power degradation follows multi-stage thermal aging, each stage with distinct time dependence.

The curve fitting results also show that the higher-temperature, higher-SOC aging (e.g. 100% SOC at 45 and 55 °C, and 80% SOC at 55 °C) behaved differently from the rest, as indicated by the disappearance of a "middle transition stage." In contrast, the lower the temperature and SOC, the middle-stage transition becomes more noticeable. The progression with logarithmic time scale also suggests that the processes are most likely related to reaction kinetics (such as charge transfer or chemical reaction rate), not mass transport.

The amount of power fade (in a logarithmic scale) averaged over cells tested under the same condition was then plotted against the reciprocal temperature (at which they were aged), according to the Arrhenius equation. Such plots are presented in Fig. 3 for three SOCs, respectively. Each plot displays the progression of the Arrhenius curves with aging intervals (or RPTs). Least-square linear curve fitting was applied to yield a slope for each curve, which was then
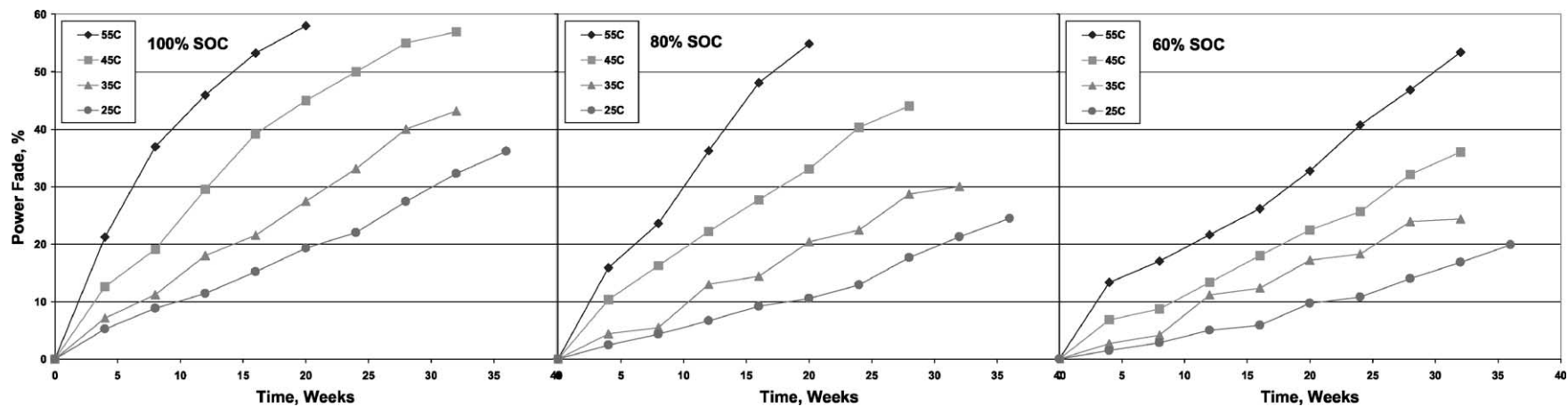
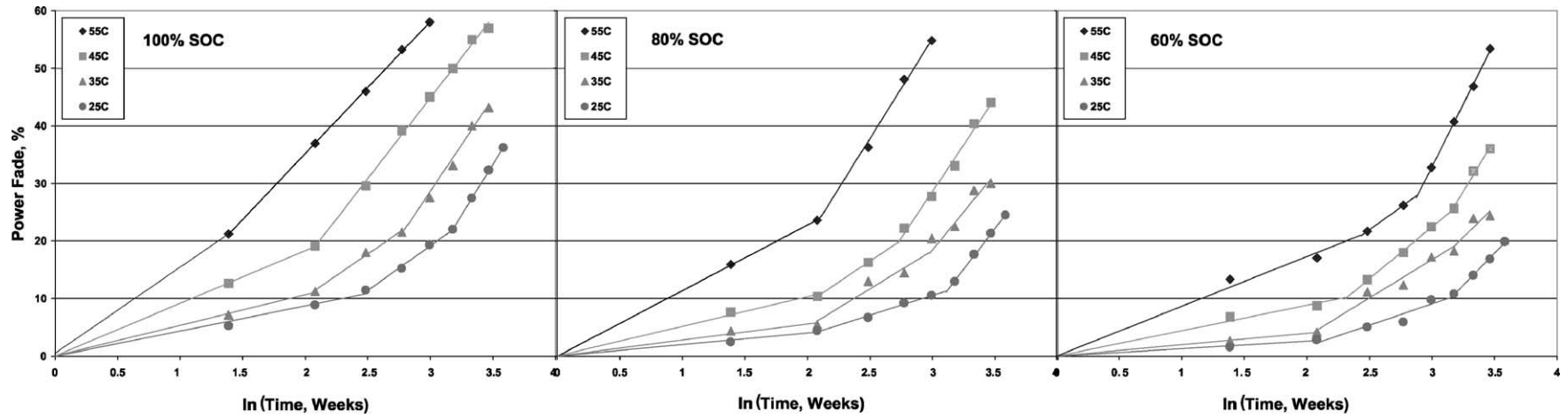Fig. 1. Time- and temperature-dependent power degradation in the GEN 2 cells through thermal aging at different SOCs.

Fig. 2. Multi-stage power degradation in the GEN 2 cells through thermal aging at different SOCs.
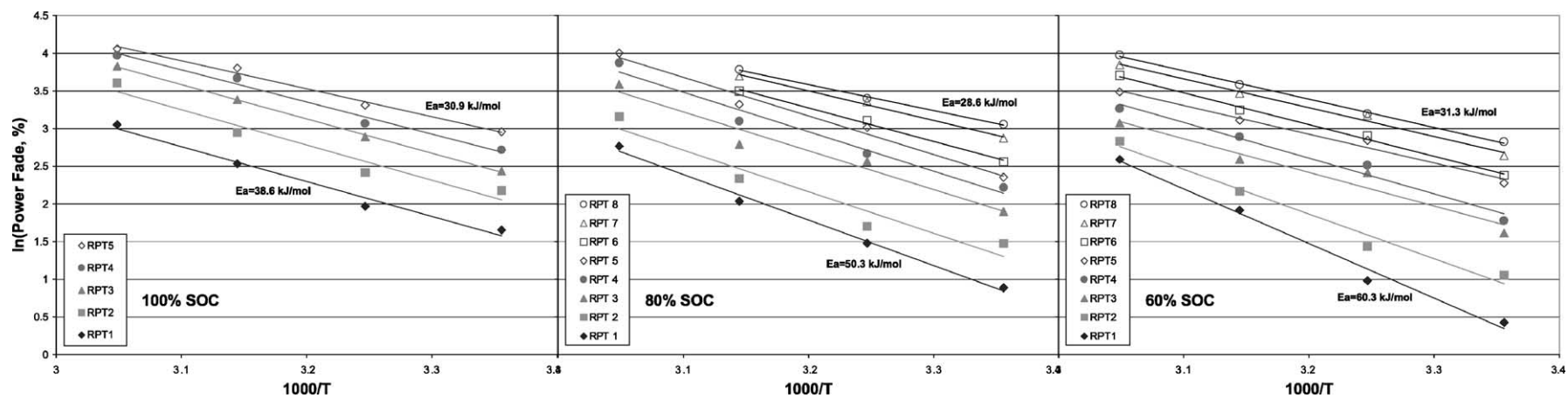
Fig. 3. Arrhenius plots of power fade vs. reciprocal temperature according to the Arrhenius equation representing logarithmic power capability loss (PCL) in watts with temperature for cells aged at three SOCs. The slope of each curve represents the gross (or apparent) activation energy related to the power fade at each stage of life. The values for RPT1 (4 weeks), RPT5 (20 weeks, for 100% SOC) and RPT8 (32 weeks, for 80 and 60% SOCs) are shown.
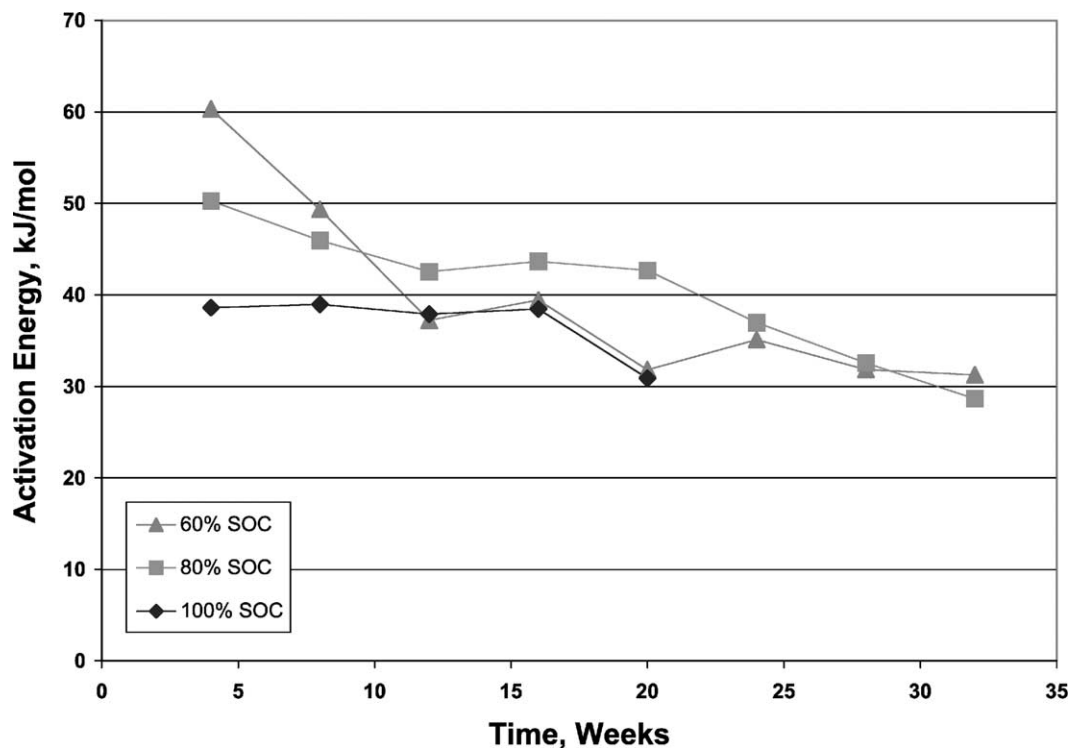
Fig. 4. Activation energy values determined from the power fade Arrhenius curves as a function of time and SOC, showing distinct changes with time and stage of degradation.

used to derive the activation energy for each stage of degradation. The activation energy values for each SOC as a function of aging interval are shown in Fig. 4. Our discussion will focus on 80% SOC data, due to limited information obtained from the microcalorimetry measurements.

In the beginning of aging, the cells aged at 80% SOC degraded with a thermally activated process exhibiting descending activation energy values, from 50.3 kJ/mol at the end of the 4th week interval to 42.5 kJ/mol at the end of the 12th week interval. The value stays in a narrow range of 43.1 ± 0.6 kJ/mol between the 12th and 20th week intervals and then begin to descend, reaching 28.6 kJ/mol at the end of the 32nd week interval. The trend of changes in the activation energy values coincide with the trend of changes in the power fade degradation behavior, as depicted in Fig. 2 for 80% SOC cells.

Figs. 5 and 6 show C_1 and C_{25} capacity fade, respectively, by thermal aging for three different SOCs. The C_{25} capacity fade is generally less then the C_1 fade. The difference however disappears as temperature and SOC decrease.

Figs. 7 and 8 illustrate the trend of C_1 and C_{25} capacity fade, respectively, over the 36-week period of aging for three SOCs. A multi-stage behavior, more or less coincides with the power fade trend, is also observed. The Arrhenius plots of both C_1 and C_{25} for cells aged at 80% SOC are given in Fig. 9. In the figure, we noticed that the 25 °C data

behave differently from the higher temperature counterparts. By excluding them from linear curve fittings, we obtained more consistent linear fit for data over the 35–55 °C range on each RPT curve. Thus, we yield an activation energy for the higher temperature degradation in C_1 and C_{25} fades after each aging interval. The results are summarized in Fig. 10, where the change of activation energy for C_1 and C_{25} fade respectively is shown with aging intervals. Due to limited data sets available for such analyses, only the first five RPTs are derived and shown. Interestingly, the first three values derived from C_1 fade are very similar to those derived from the power fade, implying the same origin in the first stage of thermal degradation. Between the 12th and the 20th week intervals, the activation energy values derived from the C_{25} fades coincide with those from the power fade, again, suggesting that they might come from the same origin in the "middle transition stage" of aging.

Fig. 11 displays an interfacial impedance change in a cell after 12 weeks of aging at 80% SOC. The slope derived from the interfacial impedance yields an activation energy of 32.2 kJ/mol, a value very close to those derived from the C_{25} fades in the first stage of degradation, as shown in Fig. 10.

Fig. 12 shows microcalorimetry results obtained from two cells at 80% SOC that have not been subjected to thermal aging. The static heat generation rates from the cells were measured in the microcalorimeter at five different
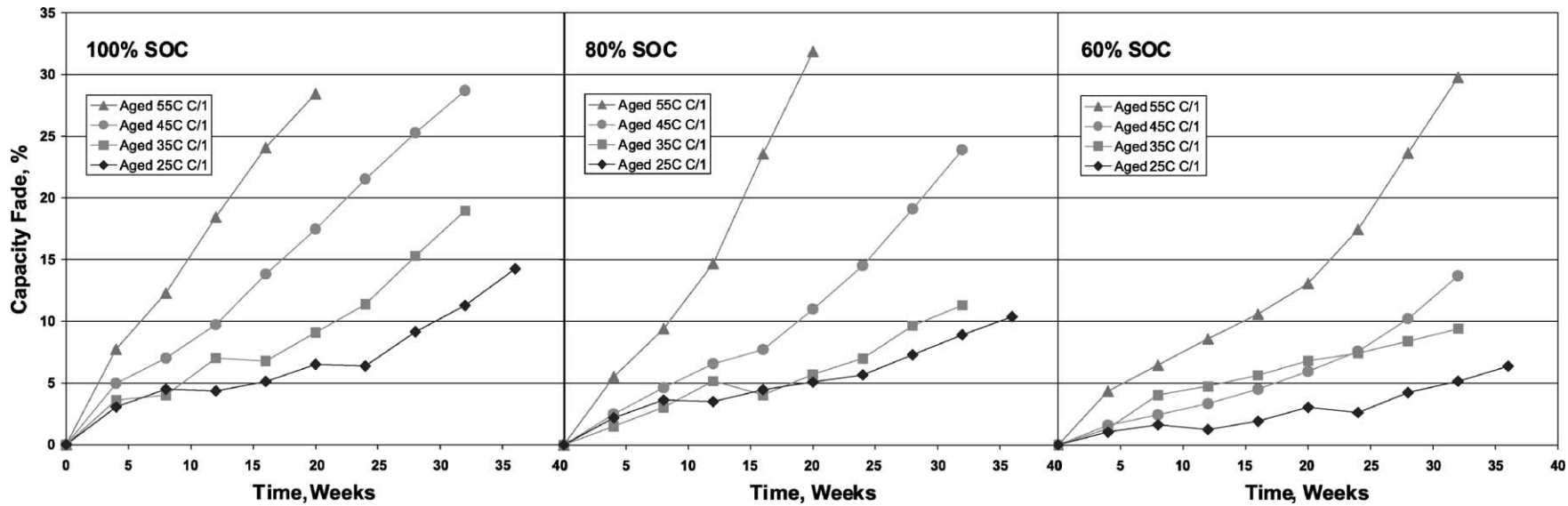
Fig. 5. C_1 capacity fade showing time- and temperature-dependent degradation similar to the trend in power fade.
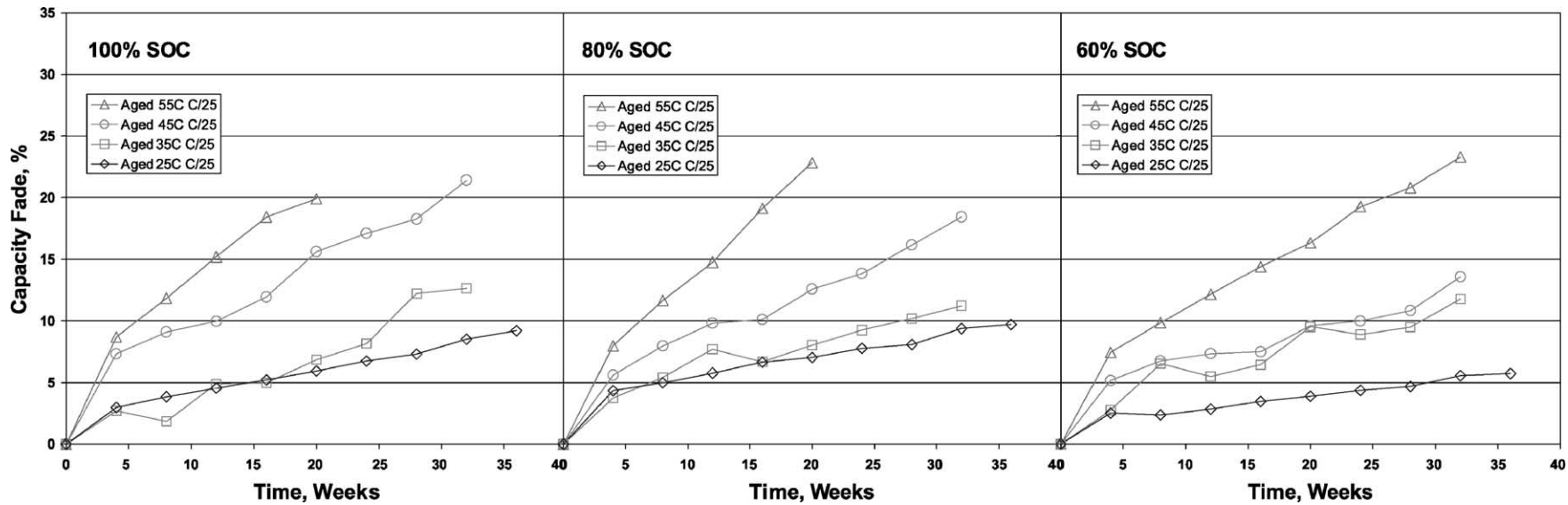
Fig. 6. C_{25} capacity fade showing different time- and temperature-dependences in degradation.
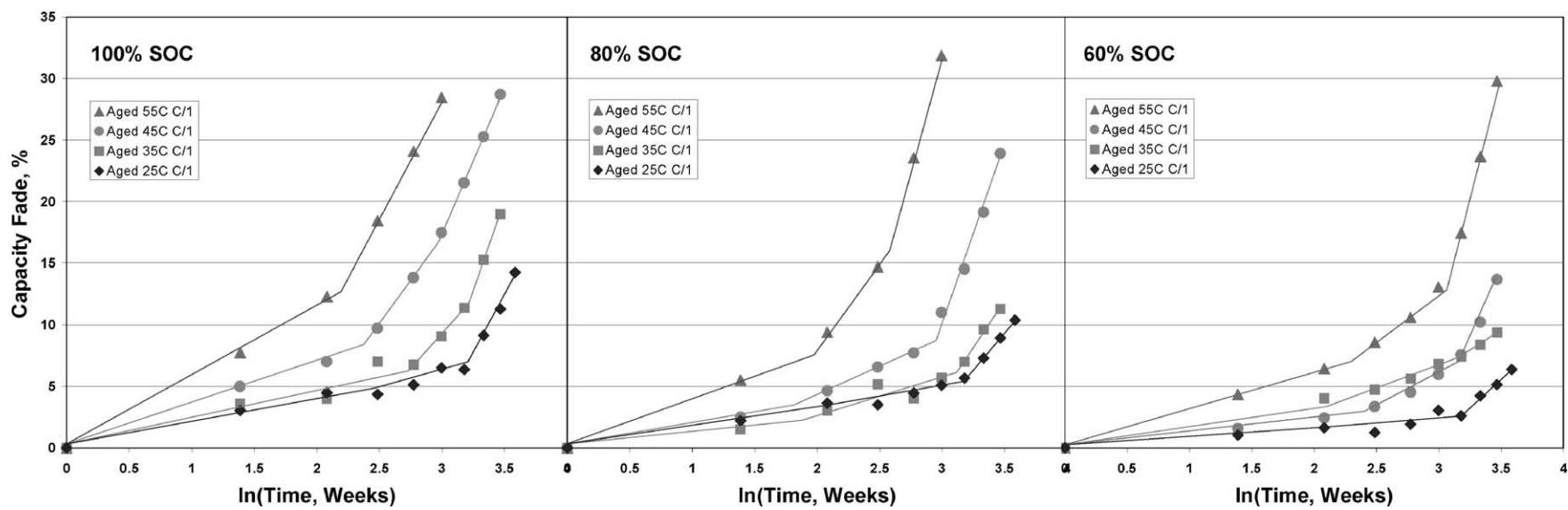
Fig. 7. Multi-stage C_1 capacity fade as a function of logarithmic time and aging temperature at three different SOCs.
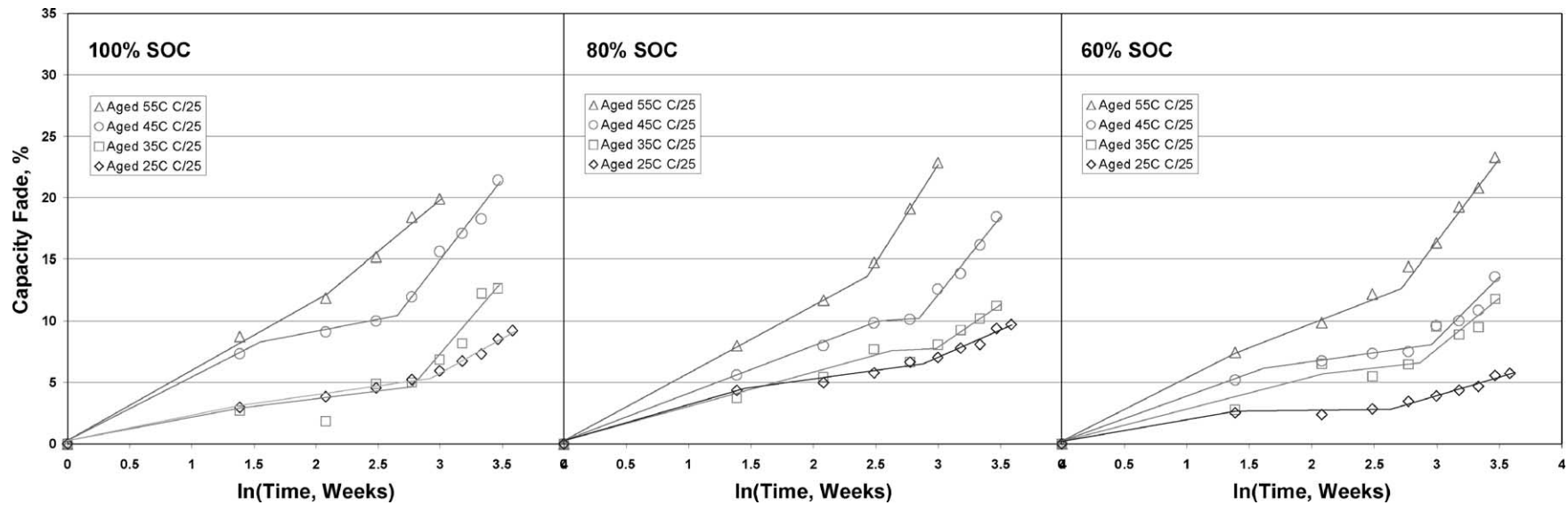
Fig. 8. C_{25} capacity fade also shows multi-stage degradation as a function of logarithmic time and aging temperature at three different SOCs. The trend lines are however different from those of the C_1 capacity fade.
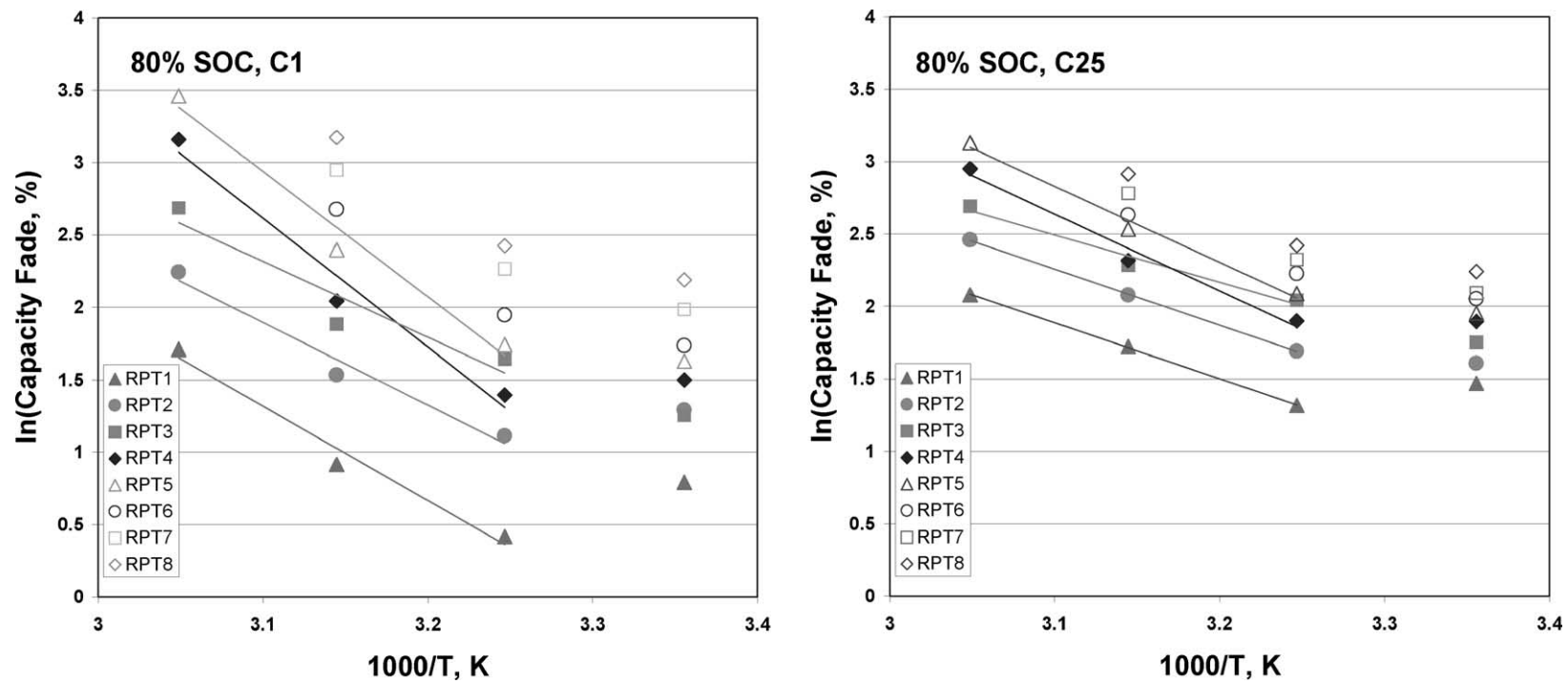
Fig. 9. Arrhenius plots of logarithmic capacity fades, C_1 and C_{25}, respectively, vs. reciprocal temperature for cells aged at 80% SOC.
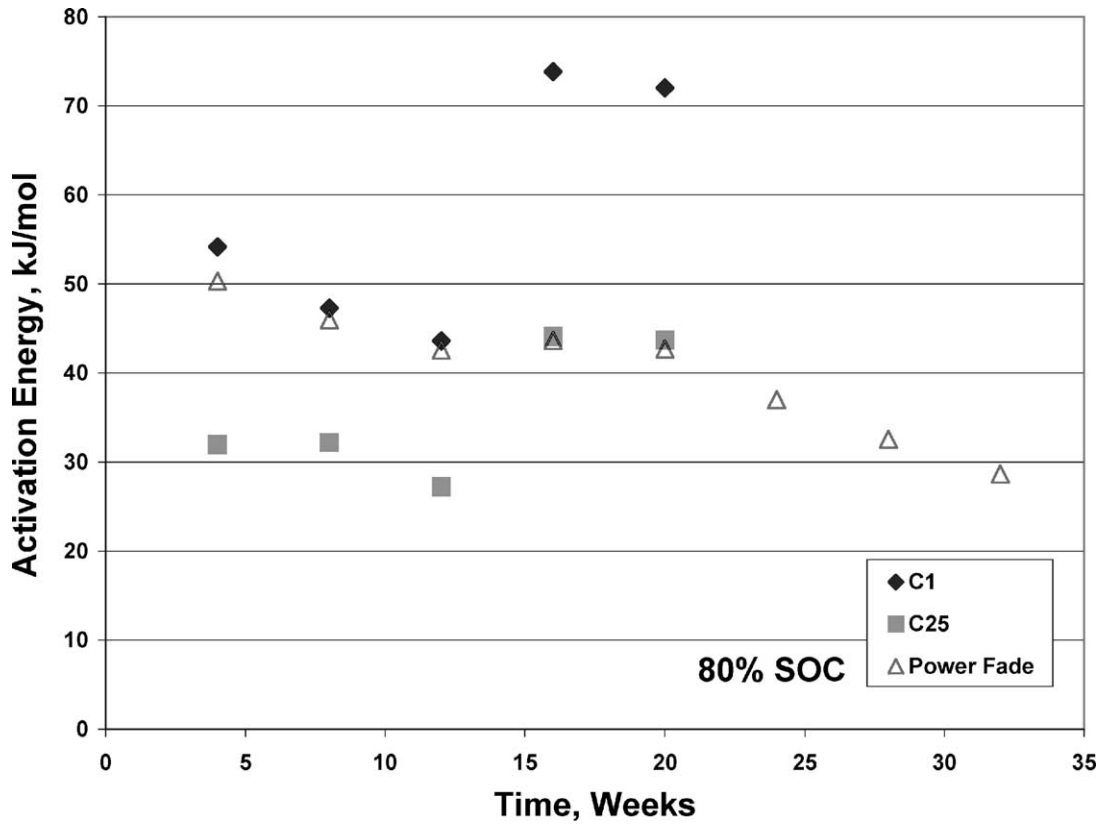
Fig. 10. Activation energy related to the C_1 and C_{25} capacity fades change with aging time for cells aged at 80% SOC. The activation energy values are derived from the slopes corresponding to the 35–55 °C range. Only first five RPTs are shown. The 80% SOC power fade data shown in Fig. 4 are also included for comparison.

temperatures from 25 to 65 °C. The resulting heat in microwatts (μW) is shown in logarithmic scale against reciprocal temperature. The result is a linear dependency depicting a constant Arrhenius activation energy of the order of 48.0

and 61.8 kJ/mol, respectively. The mean value of 54.9 kJ/mol surprisingly resembles to those observed in the first stage of degradation derived from the power and C_1 capacity fades.
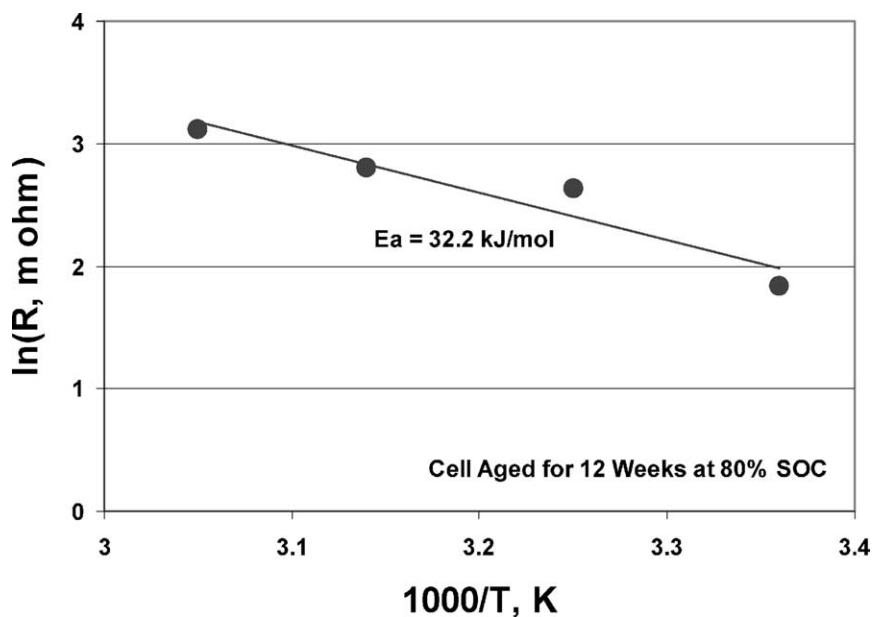

Fig. 11. Arrhenius plot and activation energy derived from the interfacial impedance change of a cell aged at 80% SOC for 12 weeks.
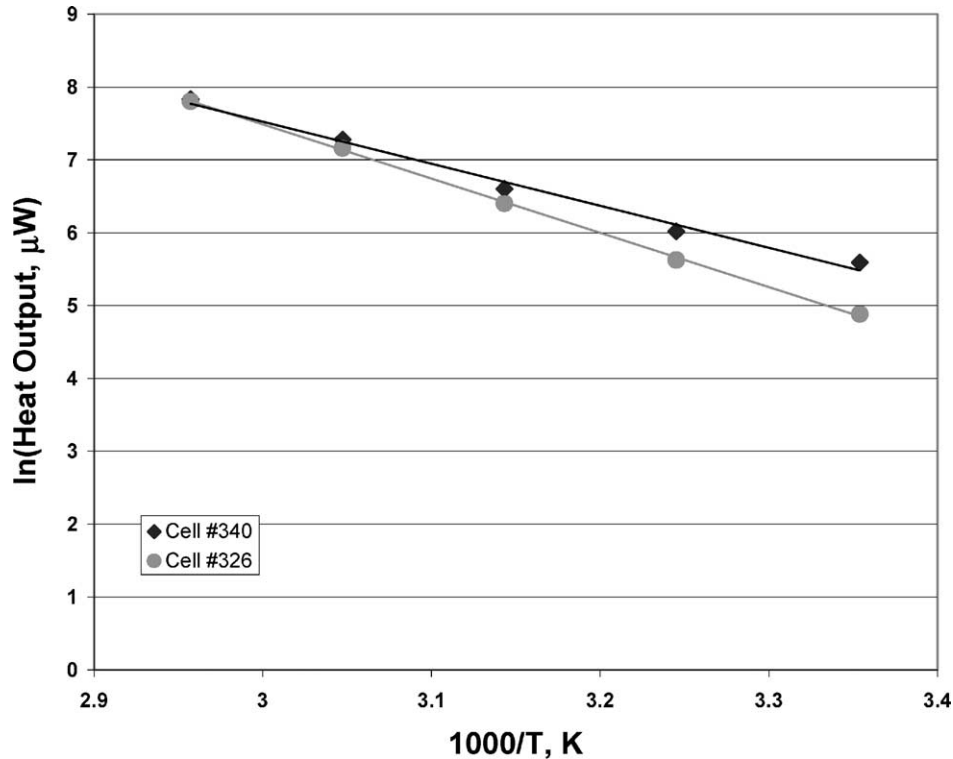
Fig. 12. Arrhenius plot showing the static heat generation rate measured from microcalorimetry on unaged cells at 80% SOC.

4. Conclusion

This paper reports on the Arrhenius analysis of the GEN 2 cells undergoing various aging conditions at different temperatures and SOCs. The changes of power capability, rate capacity, and impedance with aging conditions were investigated in the accelerated life tests. The degradation follows a multi-stage process with a middle transition stage shown in cells subjected to lower temperature aging. The changes of these properties with temperature, as depicted by Arrhenius equations, were analyzed and correlation among these properties was sought. In addition, microcalorimetry has also been performed on two unaged cells at 80% SOC to study static heat generation across a comparable temperature range of 25–65 °C. We found that the activation energy derived from the Arrhenius analyses on power fade, C_1 capacity fade, and static heat generation all yielded a similar value of the order of 50–55 kJ/mol in the initial stage of degradation, suggesting that they might come from the same origin. On the other hand, the correlation between the activation energy derived from the interfacial impedance change and C_{25} capacity fade yielded a similar value of the order of 32 kJ/mol, implying that they might be related. The activation energy derived from the power fade and the C_{25} capacity fade yielded a similar value of the order of 43 kJ/mol in the middle transition stage, suggesting that they might follow the same degradation mechanism.

Acknowledgements

References

[1] R.G. Jungst, et al., in: Proceedings of the 40th Power Sources Conference, Cherry Hill, NJ, 10–13 June 2002.
[2] (a) PNGV Battery Test Manual, DOE/ID-10597, Revision 3, February 2001;
(b) PNGV Test Plan for Advanced Technology Development GEN 2 Lithium-ion Cells, EHV-TP-121, INEEL, Revision 4, June 2001.